(Nitro)Iron(III) Porphyrins. EPR Detection of a Transient Low-Spin Iron(III) Complex and Structural Characterization of an O Atom Transfer Product

Orde Q. Munro and W. Robert Scheidt*

The Department of Chemistry and Biochemistry, University of Notre Dame, Notre Dame, Indiana 46556

Received July 8, 1997

The reaction of $BF_3{\cdot}OEt_2$ with the bis(nitro) complex of iron(III) picket-fence porphyrin, $[K(18C6)(OH_2)][Fe(TpivPP)(NO_2)_2]$, leads to the formation of a transient porphyrin intermediate, assigned on the basis of its rhombic low-spin EPR spectrum as the five-coordinate N-bound mono(nitro) iron(III) derivative, $[Fe(TpivPP)(NO_2)]$. This species is reactive and readily undergoes oxygen atom transfer to form $[Fe^{III}(TpivPP)(NO_3)]$ and $[Fe^{II}(TpivPP)(NO)]$. The reactions have been followed by EPR and IR spectroscopy. $[Fe(TpivPP)(NO_2)]$ has a rhombic EPR spectrum (g = 2.60, 2.35, and 1.75) in chlorobenzene and CH_2Cl_2 and is spectroscopically distinct from the bis(nitro) starting material (g = 2.70, 2.50, and 1.57). Oxidation of the nitrosyl species to $[Fe(TpivPP)(NO_3)]$ proceeds via an intermediate assigned as $[Fe(TpivPP)(NO_2)]$ on the basis of its EPR spectrum. The crystal structure of one of the reaction products, $[Fe(TpivPP)(NO_3)]$, has been determined. The nitrate ion of $[Fe(TpivPP)(NO_3)]$ is bound to the iron(III) ion in a "symmetric" bidentate fashion within the ligand-binding pocket of the porphyrin pickets. Individual Fe−O distances are 2.123(3) and 2.226(3) Å. The dihedral angle between the plane of the nitrate ion and the closest N_p−Fe−N_p plane is 10.0°. The Fe−N_p bonds (and trans N_p−Fe−N_p angles) perpendicular and parallel to the plane of the axial ligand average to 2.060(5) Å (154.84(9)°) and 2.083(3) Å (146.14(9)°), respectively. Crystal data for $[Fe(TpivPP)(NO_3)]$: a = 23.530(2) Å, b = 10.0822(5) Å, c = 48.748(3) Å, β = 92.145(5)°, monoclinic, space group $I2/a$, V = 11556.4(14) Å^3, Z = 8, $FeN_9O_7C_{64}H_{64}$, 8798 observed data, R_1 = 0.0606, wR_2 = 0.1313, all observations at 127(2) K.

Introduction

Nitric oxide (NO), nitrite (NO_2^-), and nitrate (NO_3^-) are three metabolically linked oxides of nitrogen found in the tissues and organs of living organisms.[1] Nitric oxide is produced *in vivo* in mammals by heme-containing nitric oxide synthases from L-arginine and functions as a smooth muscle relaxant, modulating vascular tone in endothelial tissues and synaptic plasticity in neural tissues.[2] However, nitric oxide has a short half-life[3] and is rapidly metabolized to nitrite and nitrate;[4] the latter is excreted in urine and may be used to gauge total NO synthase activity.[5] One mechanism that has been proposed for the oxidation of NO to nitrate *in vivo* involves hemoglobin. Specifically, NO released from cells into the blood is bound by ferrous hemoglobin to form HbNO[6] which is then oxidized to NO_3^- by molecular oxygen.[1] Kinetic studies on the oxidation of MbNO are in agreement with this mechanism.[7] Free NO also reacts with the dioxygen complexes of ferrous Hb and Mb to form the corresponding high-spin iron(III) hemoproteins and NO_3^-.[8] Nitrite ion is known to interact with several hemoproteins. The reaction of NO_2- with oxyhemoglobin *in vivo* results in stoichiometric formation of nitrate and methemoglobin.[5,9] Nitrite is also the substrate of assimilatory nitrite reductases which contain an isobacteriochlorin prosthetic group (siroheme) and an Fe_4S_4 cluster and catalyze the six-electron reduction of nitrite ion to ammonia.[10] The reduced hemoprotein binds nitrite ion to form an iron(II)−nitrosyl complex which is also observed as a steady state intermediate in the catalytic cycle of the enzyme.[11] The dissimilatory nitrite reductases contain two *c*-type and two d_1-type hemes (dioxoisobacteriochlorins)[12] and reduce nitrite ion to nitrous oxide, nitric oxide, or dinitrogen.[13] Commercially, ascorbate reduction of metMb coupled with

* To whom correspondence should be addressed. Electronic mail: Scheidt.1@nd.edu.

(1) Inoue, M.; Minamiyama, Y.; Takemura, S. *Methods Enzymol.* **1996**, *269*, 474.
(2) (a) Hibbs, J. B., Jr.; Vavrin, Z.; Taintor, R. R. *J. Immunol.* **1987**, *138*, 550. (b) Hibbs, J. B., Jr.; Taintor, R. R.; Vavrin, Z. *Science* **1987**, *235*, 473. (c) Lyengar, R.; Stuehr, D. J.; Marletta, M. A. *Proc. Natl. Acad. Sci. U.S.A.* **1987**, *84*, 6369.
(3) (a) Palmer, R. M. J.; Ashton, D. S.; Moncada, S. *Nature (London)* **1988**, *333*, 664. (b) Marletta, M. A.; Yoon, P. S.; Lyengar, R.; Leaf, C. D.; Wishnok, J. S. *Biochemistry* **1988**, *27*, 8706.
(4) (a) Granger, D. L.; Hibbs, J. B., Jr.; Broadnax, L. M. *J. Immunol.* **1991**, *146*, 1294. (b) Hibbs, J. B., Jr.; Westenfelder, C.; Taintor, R. R.; Vavrin, Z.; Kablitz, C.; Baranowski, R. L.; Ward, J. H.; Menlove, R. L.; McMurry, M. P.; Kushner, J. P.; Samlowski, W. E. *J. Clin. Invest.* **1992**, *89*, 867.
(5) Granger, D. L.; Taintor, R. R.; Boockvar, K. S.; Hibbs, J. B., Jr. *Methods Enzymol.* **1996**, *268*, 142.
(6) Abbreviations: 18C6, 1,4,7,10,13,16-hexaoxacyclooctadecane; DMF, *N, N*′-dimethylformamide; K(222), potassium complex of 4,7,13,16,-21,24-hexaoxa-1,10-diazabicyclo[8.8.8]hexacosane; Mb, ferrous myoglobin; metMb, ferric myoglobin; OEP, dianion of 2,3,7,8,12,13,17,18-octaethylporphyrin; TPP, dianion of 5,10,15,20-tetraphenylporphyrin; TpivPP, dianion of α,α,α,α -tetrakis(*o*-pivalamidophenyl)porphyrin.
(7) Arnold, E. V.; Bohle, D. S. *Methods Enzymol.* **1996**, *269*, 41.
(8) Eich, R. F.; Li, T.; Lemon, D. D.; Doherty, D. H.; Curry, S. R.; Aitken, J. F.; Mathews, A. J.; Johnson, K. A.; Smith, R. D.; Phillips, G. N., Jr.; Olson, J. S. *Biochemistry* **1996**, *35*, 6976.
(9) Kosaka, H.; Imaizumi, K.; Imai, K.; Tyuma, I. *Biochim. Biophys. Acta* **1979**, *581*, 184.
(10) (a) Vega, J. M.; Kamin, H. *J. Biol. Chem.* **1977**, *252*, 896. (b) Aparicio, P. J.; Knaff, D. B.; Malkin, R. *Arch. Biochem. Biophys.* **1975**, *169*, 102. (c) Coleman, K. J.; Cornish-Bowden, A.; Cole, J. A. *Biochem. J.* **1978**, *175*, 483.
(11) Lancaster, J. R.; Vega, M. J.; Kamin, H.; Orme-Johnson, N. R.; Orme-Johnson, W. H.; Krueger, R. J.; Siegel, L. M. *J. Biol. Chem.* **1979**, *254*, 1268.
(12) Chang, C. K. *J. Biol. Chem.* **1985**, *260*, 9520.

S0020-1669(97)00855-0 CCC: $15.00
Published on Web 04/15/1998

coordination of nitrite ion forms the basis of cured meat preservation and coloration.[14]

Over the past decade, several studies on iron(III) porphyrins in nonaqueous media in the presence of nitrite ion have appeared. Fernandes et al.[15] reported spectroscopic evidence for stepwise formation of [Fe(TPP)(NO_2)] and [Fe(TPP)(NO_2)$_2$]$^-$ in DMF, with the five-coordinate low-spin N-bound nitro complex apparently stable under these conditions. However, we found that the addition of nitrite ion to a solution of [Fe(TPP)($OClO_3$)] in DMF produced the corresponding Fe(II)−NO complex rather than [Fe(TPP)(NO_2)] or [Fe(TPP)(NO_2)$_2$]$^-$.[16] Furthermore, formation of the iron(II) nitrosyl species was accompanied by formation of the corresponding nitrato complex, particularly at low nitrite/(porphinato)iron(III) ratios. More recently, Castro et al.[17] reported that [Fe(OEP)Cl] stoichiometrically inserts oxygen into substrates with allylic, benzylic, and aldehydic C−H bonds in the presence of a slight excess (2−4 equiv) of NO_2^-. Other substrates similarly oxidized included NO, O_2, CO, Ph_3P, and Me_2S.[18] Formation of [Fe^{II}(OEP)(NO)], which is produced by oxygen atom transfer from a species assumed to be [Fe(OEP)(NO_2)], apparently drives the reaction thermodynamically.[17] Frangione et al.[19] have recently published the visible spectrum of a species assigned as [Fe(TpivPP)(NO_2)] in acetonitrile. However, their equilibrium model analysis of the NO_2^- binding equilibria suggested that the "mono(nitro)" complex was in fact the six-coordinate mixed-ligand species, [Fe(TpivPP)(NO_2)(ClO_4)]$^-$.

Our earlier studies with [Fe(TPP)($OClO_3$)][16] and those of Castro and co-workers with [Fe(OEP)Cl][17] suggest that, under conditions which favor a nonzero concentration of the *five-coordinate* (nitro)iron(III) species (low nitrite ion concentration), oxygen atom transfer from iron-bound nitrite to a variety of substrates, including NO_2^-,[16] occurs. This behavior appears to be more limited in the presence of a large excess of nitrite ion, particularly with sterically hindered porphyrins such as picket-fence porphyrin[20] (and [K(18C6)]$^+$ as the counterion), since we have been able to isolate and structurally characterize the bis(nitro) iron(III) complex, [K(18C6)(H_2O)][Fe(TpivPP)(NO_2)$_2$].[21] However, the controversial question of whether a *bona fide* mono(nitro) iron(III) porphyrin is stable enough to be isolated and spectroscopically and/or structurally characterized clearly remains unanswered.

In the present work, we have specifically attempted to synthesize the sterically protected five-coordinate N-bound mono(nitro) iron(III) complex, [Fe(TpivPP)(NO_2)]. We have used EPR spectroscopy to characterize the reaction system. Our EPR data show the presence of an intermediate, possibly the desired five-coordinate mono(nitro) iron(III) complex which is a low-spin species and probably N-bound. Although the porphyrin picket groups provide some protection for the $Fe^{III}-NO_2^-$ moiety, this species is unstable and oxygen atom transfer occurs, yielding [Fe(TpivPP)(NO_3)] and [Fe(TpivPP)(NO)] as final products. The molecular structure of [Fe(TpivPP)(NO_3)] has been determined from low-temperature X-ray diffraction data.

Experimental Section

General Information. All manipulations, except oxidation reactions, were carried out under argon using a double-manifold vacuum line, Schlenkware, and cannula techniques. Chloride ion was removed from chlorobenzene by washing with sulfuric acid prior to drying by distillation over P_2O_5. Methylene chloride and pyridine were distilled over CaH_2, and hexanes over sodium benzophenone. Boron trifluoride etherate (Fisher) was distilled from a slight excess of diethyl ether over CaH_2 immediately before use.[22] KNO_2 (Fisher) was recrystallized twice from distilled water, dried overnight at 75 °C, and stored under argon. 18-Crown-6 (Aldrich) was recrystallized from CH_3CN and dried under vacuum. The free base porphyrin, *meso*-α,α,α,α-tetrakis(*o*-pivalamidophenyl)porphyrin (H_2 TpivPP), and the corresponding chloro and triflate iron(III) derivatives were synthesized using literature procedures.[20,23] [K(18C6)(OH_2)][Fe(TpivPP)(NO_2)$_2$] was prepared from [Fe(TpivPP)(OSO_2CF_3)(OH_2)] using the method described by Nasri et al.[21]

Electronic spectra were recorded with Perkin-Elmer Lambda 19 or Lambda 6 spectrometers using chlorobenzene or methylene chloride solutions in 1.0 and 0.1 cm pathlength cuvettes. IR spectra were recorded with a Perkin-Elmer Model 883 spectrometer as Nujol mulls on CsBr disks or as KBr pellets. EPR spectra were recorded at 77 K with X-band Varian E-12 and Bruker ER 100E spectrometers. The magnetic field was calibrated with an external DPPH standard (g = 2.0037). Solid samples were ground single crystals; frozen solution spectra were obtained in chlorobenzene, methylene chloride, and DMF. Freshly opened bottles of DMF were used, but no further attempts were made to dry this solvent for EPR spectroscopy.

Attempted Synthesis of [Fe(TpivPP)(NO_2)] from [Fe(TpivPP)(NO_2)(Py)]. [Fe(TpivPP)(NO_2)(Py)] was prepared from [K(18C6)(OH_2)][Fe(TpivPP)(NO_2)$_2$] using an excess of pyridine in dry chlorobenzene as described previously.[24] Attempts to remove iron-bound pyridine from single crystals of [Fe(TpivPP)(NO_2)(Py)] under vacuum (<0.05 mmHg) overnight were unsuccessful; the EPR spectrum of several crushed crystals remained unchanged ([Fe(TpivPP)(NO_2)(Py)]; g_1 = 2.94, g_2 = 2.36, g_3 = 1.36).[24] Finely ground (powder) samples of [Fe(TpivPP)(NO_2)(Py)] were equally inert to pyridine loss under vacuum (<0.05 mmHg), both after 14 h at ambient temperature and after 16 h at 73 °C. However, partial decomposition of [Fe(TpivPP)(NO_2)(Py)] to form a high-spin product ($g_\perp$ = 5.66) and an {FeNO}^{7} species, [Fe(TpivPP)(NO)] (g_3 = 2.01, $a_3 \approx$ 16 G), was observed after 16 h at 73 °C.[25,26]

Reaction of [K(18C6)(OH_2)][Fe(TpivPP)(NO_2)$_2$] with BF_3·OEt_2. To 28.1 mg (19 μmol) of dry, powdered [K(18C6)(OH_2)][Fe(TpivPP)-

(13) (a) Firestone, M. K.; Firestone, R. B.; Tiedje, J. M. *Biochem. Biophys. Res. Commun.* **1979**, *91*, 10. (b) Johnson, M. K.; Thomson, A. J.; Walsh, T. A.; Barber, D.; Greenwood, C. *Biochem. J.* **1980**, *189*, 285.
(14) (a) Tsukahara, K.; Yamamoto, Y. *J. Biochem. (Tokyo)* **1983**, *93*, 15. (b) Fox, J. B.; Thomson, J. S. *Biochemistry* **1963**, *2*, 465. (c) Giddings, G. G. *J. Food Sci.* **1977**, *42*, 288. (d) Cassens, R. G.; Greaser, M. L.; Ito, T.; Lee, M. *Food Technol.* **1979**, *33*, 46.
(15) Fernandes, J. B.; Feng, D. W.; Chang, A.; Keyser, A.; Ryan, M. D. *Inorg. Chem.* **1986**, *25*, 2606.
(16) Finnegan, M. G.; Lappin, A. G.; Scheidt, W. R. *Inorg. Chem.* **1990**, *29*, 181.
(17) (a) O'Shea, S. K.; Wang, W.; Wade, R. S.; Castro, C. E. *J. Org. Chem.* **1996**, *61*, 6388. (b) Castro, C. E.; O'Shea, S. K. *J. Org. Chem.* **1995**, *60*, 1922.
(18) In the case of the putative five-coordinate (nitro)iron(III) complex [Fe(OEP)(NO_2)], dioxygen appears to be reversibly oxidized by direct O atom transfer from N-bound nitrite: (OEP)$Fe^{III}NO_2 + O_2 \rightleftharpoons$ (OEP)Fe^{II}-NO + O_3.[17a]
(19) Frangione, M.; Port, J.; Baldiwala, M.; Judd, A.; Galley, J.; DeVega, M.; Linna, K.; Caron, L.; Anderson, E.; Goodwin, J. A. *Inorg. Chem.* **1997**, *36*, 1904.
(20) Collman, J. P.; Gagne, R. R.; Halbert, T. R.; Lang, G.; Robinson, W. T. *J. Am. Chem. Soc.* **1975**, *97*, 1427.
(21) Nasri, H.; Goodwin, A.; Scheidt, W. R. *Inorg. Chem.* **1990**, *29*, 185.
(22) Fieser, L. F.; Fieser, M. *Reagents for Organic Synthesis*; John Wiley & Sons: New York, 1967; Vol. 1, p 70.
(23) Gismelseed, A.; Bominaar, E. L.; Bill, E.; Trautwein, A. X.; Nasri, H.; Doppelt, P.; Mandon, D.; Fischer, J.; Weiss, R. *Inorg. Chem.* **1990**, *29*, 2741.
(24) Nasri, H.; Wang, Y.; Huynh, B. H.; Walker, F. A.; Scheidt, W. R. *Inorg. Chem.* **1991**, *30*, 1483.
(25) The {MNO}^{n} notation is that of Enemark and Feltham: Enemark, J. H.; Feltham, R. D. *Coord. Chem. Rev.* **1974**, *13*, 339. *n* corresponds to the number of d electrons plus the unpaired electron of the NO ligand.
(26) Given the nature of the product mixture observed by EPR spectroscopy, no attempt was made to obtain a DSC thermogram of pyridine thermolysis from [Fe(TpivPP)(NO_2)(Py)].

$(NO_2)_2$] in a Schlenk tube under argon was added ~4 mL of chlorobenzene and 3.0 μL (24 μmol) of freshly distilled BF_3·OEt_2. The deep red solution turned red-brown on swirling at ambient temperature. The EPR spectrum of a reaction mixture aliquot drawn after 25 min indicated the coexistence of three species: a high-spin species with a signal at $g = 5.57$ (with a slight shoulder to lower field, $g \approx 7.6$), a low-spin species with $g_1 = 2.60$, $g_2 = 2.37$, and $g_3 \approx 1.7$, and a nitrosyl species with an anisotropic signal centered around $g \approx 2.06$ ($g_3 = 2.01$, $a_3 \approx 17$ G). After 48 h, the chlorobenzene solution was layered with hexanes and crystallization was allowed to proceed in the dark; X-ray-quality crystals formed after 3 days. A low-temperature X-ray diffraction study revealed that one crystalline reaction product was [Fe(TpivPP)(NO_3)]. UV−vis (C_6H_5Cl): λ_{max}, nm (ϵ, M^{-1} cm^{-1}) 349 (2.60×10^4), 415 (7.55×10^4), 509 (9.0×10^3), 574 (3.4×10^3), 639 (2.0×10^3), 671 (1.7×10^3). IR (C_6H_5Cl): ν (NO_3) 1520 cm^{-1} (s), 1250 cm^{-1} (br), 1047 cm^{-1} (m). IR (KBr pellet): ν(NO_3) 1515 cm^{-1} (s), 1255 cm^{-1} (br), 1072 cm^{-1} (m).

EPR Study of the Reaction of [K(18C6)(OH_2)][Fe(TpivPP)$(NO_2)_2$] with BF_3·OEt_2. All Schlenk and EPR tubes were cooled to 2 ± 2 °C in ice−water baths, and solution transfers were carried out under argon using cannula techniques. In a typical reaction, 3.7 μL (30 μmol) of freshly distilled BF_3·OEt_2 was injected into 7.6 mL of dry chlorobenzene and the system allowed to attain thermal equilibrium. The reaction was started by transferring the chlorobenzene solution of BF_3·OEt_2 to a second Schlenk tube containing 34.1 mg (23 μmol) of powdered [K(18C6)(OH_2)][Fe(TpivPP)$(NO_2)_2$]. Samples for EPR spectroscopy (~60−70 μL) were withdrawn from the reaction mixture at set time intervals (up to 25.7 h) and, upon complete transfer, immediately frozen in liquid nitrogen. An EPR spectrum of the reaction mixture at t_∞ was obtained after maintaining the solution at 4 °C for 10 days under argon. The reaction was also studied in CH_2Cl_2 and DMF.

Oxidation Studies. [Fe(TpivPP)(NO)] produced in the reaction of [K(18C6)(OH_2)][Fe(TpivPP)$(NO_2)_2$] with BF_3·OEt_2 could be oxidized in air or with pure oxygen. [K(18C6)(OH_2)][Fe(TpivPP)$(NO_2)_2$] (32.5 mg, 22.0 μmol) was dissolved in ~7 mL of chlorobenzene under argon, and 3.2 μL (25.9 μmol) of BF_3·OEt_2 was added. The solution was stirred at 40 °C under argon overnight. An aliquot of the reaction mixture was withdrawn for EPR spectroscopy (t_0 sample), prior to passing pure oxygen through the solution at 40 °C (stainless steel needle) and periodically withdrawing and freezing additional samples.

X-ray Diffraction Study of [Fe(TpivPP)(NO_3)]. Single crystals of [Fe(TpivPP)(NO_3)] grown by slow diffusion of hexane into a chlorobenzene solution of the metalloporphyrin were flat needles. A dark purple-brown crystal with the dimensions 0.60 × 0.13 × 0.07 mm was mounted on the end of a glass fiber with its long axis approximately collinear with the axis of the fiber. All measurements were performed with graphite-monochromated Mo Kα radiation ($\bar{\lambda}$ = 0.710 73 Å) on an Enraf-Nonius FAST area detector diffractometer at 127 K as described previously.[27] Data were corrected for Lorentz and polarization factors but not for absorption ($\mu = 0.32$ mm^{-1}). A total of 36 609 observed reflections ($F_o \geq 2.0\sigma(F_o)$) were measured and averaged to 12 737 unique reflections.

The structure was solved in the monoclinic space group *I*2/*a* with the direct methods program XS,[28] as implemented in SHELXTL.[29] The E-map and subsequent difference Fourier syntheses led to the location of all non-hydrogen atoms, including those of the axial ligand. The structure was refined against F^2 using the program SHELXL-93.[30] All data collected were used including negative intensities. The metal and porphyrin non-hydrogen atoms were refined anisotropically. A difference Fourier synthesis located the eight hydrogen atoms attached to the porphyrin β carbons and most of the hydrogens of the *o*-pivalamidophenyl groups; all were included as idealized contributors in the least-squares process. Standard SHELXL-93 idealization parameters were used. At the final stages of refinement, a difference Fourier synthesis located several peaks with heights >1 e/Å^3 near C(7), C(8), C(11), and O(1), apparently due to a rotational disorder of the *o*-pivalamido group about the C(6)−N(5) bond.[31] The final refinement converged to the *R* values given in Table 1. The maximum and minimum electron densities on the final difference Fourier map were 0.61 and −0.39 e/Å^3, respectively. Complete crystallographic details, fractional atomic coordinates, anisotropic thermal parameters, bond lengths, and bond angles for [Fe(TpivPP)(NO_3)] are given in the Supporting Information (Tables S1−S6).

Table 1. Crystallographic Data for [Fe(TpivPP)(NO_3)][a]

formula	$C_{64}H_{64}FeN_9O_7$
FW, amu	1127.12
a, Å	23.530(2)
b, Å	10.0822(5)
c, Å	48.748(3)
β, deg	92.145(5)
V, Å^3	11556.4(14)
space group	*I*2/*a*
Z	8
D_c, g/cm^3	1.296
μ, mm^{-1}	0.323
radiation	Mo Kα, = 0.710 73 Å
temperature, K	127(2)
final *R* indices [$I > 2\sigma(I)$][b]	$R_1 = 0.0606$, $wR_2 = 0.1313$
final *R* indices (all data)	$R_1 = 0.0994$, $wR_2 = 0.1546$

[a] The estimated standard deviations of the least-significant digits are given in parentheses. [b] $R_1 = \Sigma||F_o| - |F_c||/\Sigma|F_o|$ and $wR_2 = \{\Sigma[w(F_o^2 - F_c^2)^2]/\Sigma[wF_o^4]\}^{1/2}$. *R* factors R_1 are based on *F*, with *F* set to zero for negative F^2. The criterion of $F^2 > 2\sigma(F^2)$ was used only for calculating R_1. *R* factors based on F^2 (wR_2) are statistically about twice as large as those based on *F*.

Results and Discussion

Nitrite ion is known to bind to [Fe(TpivPP)$(OSO_2CF_3)(OH_2)$] in a stepwise manner.[21] However, since the binding constants K_1 and K_2 are comparable in magnitude, the bis(nitro) complex is formed even at low concentrations of added nitrite ion.[21] Because of the stability of low-spin [Fe(TpivPP)$(NO_2)_2]^-$, attempts to synthesize the five-coordinate mono(nitro) iron(III) complex by direct addition of NO_2^- to a solution of [Fe(TpivPP)$(OSO_2CF_3)(OH_2)$] are unlikely to succeed. We have therefore attempted to isolate [Fe(TpivPP)(NO_2)] by (i) stoichiometric removal of pyridine from single crystals and powdered samples of the mixed-ligand complex [Fe(TpivPP)(NO_2)(Py)] and by (ii) stoichiometric removal of NO_2^- from [K(18C6)(OH_2)][Fe(TpivPP)$(NO_2)_2$] in solution. The reactions were characterized by EPR spectroscopy (IR, and electronic spectroscopy when warranted) and a structure determination of one product.

Heating samples of [Fe(TpivPP)(NO_2)(Py)] to 73 °C *in vacuo* resulted in partial loss of coordinated pyridine. However, pyridine dissociation was always accompanied by O atom transfer from iron-bound nitrite. Concomitant formation of a nitrosyl species with an anisotropic EPR signal centered around $g = 2.07$ ($g_3 = 2.01$, $a_3 \approx 16$ G) and a high-spin species ($g_\perp$ =

(27) Scheidt, W. R.; Turowska-Tyrk, I. *Inorg. Chem.* **1994**, *33*, 1314.
(28) (a) The direct methods component of the program XS implements Sheldrick's SHELX-90 "phase annealing" algorithm. Sheldrick, G. M. *Acta Crystallogr., Sect. A* **1990**, *A46*, 467.
(29) *SHELXTL*, Version 5; Siemens Industrial Automation, Inc., Analytical Instrumentation: Madison, WI, 1994; Part Number 269-015900.
(30) Sheldrick, G. M. *J. Appl. Crystallogr.*, in preparation.

(31) The disorder was resolved by allowing atoms C(10) and C(10b) to share the same site with the same anisotropic displacement parameters; idealized hydrogens were not included for either atom. Atoms C(8) and C(8b) were also constrained to have the same anisotropic displacement parameters. The atom pairs O(1)/O(1b), C(9)/C(9b), and C(11)/C(11b) were restrained to have the same U_{ij} components to within an effective standard deviation of 0.1. Idealized hydrogens were not added to C(11b). Atoms C(7) and C(7b) were similarly treated, but to within an effective standard deviation of 0.05. The site occupancy factor for the two components of the disordered *o*-pivalamido group was allowed to refine, converging to 0.839(5).

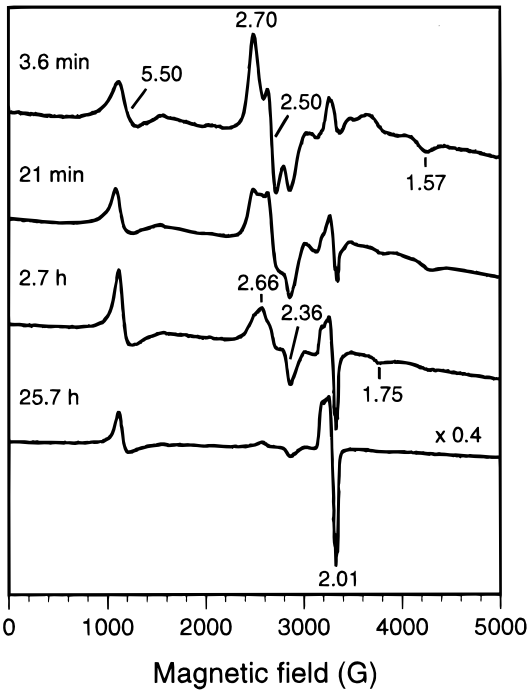

Figure 1. Selected X-band EPR spectra of samples (~60 μL) of a reaction mixture comprising a chlorobenzene solution of [K(18C6)(OH$_2$)][Fe(TpivPP)(NO$_2$)$_2$] (initial concentration 3.0 mM) and BF_3·OEt_2 (3.9 mM) at ~2 °C. The times indicated are the freezing point times after the start of the reaction.

5.7) was observed in all cases. Irreversible formation of the iron(II) nitrosyl species [Fe(TpivPP)(NO)][32] therefore appears to be favored over simple dissociation of pyridine under these conditions. The identity of the high-spin species produced in the reaction is unclear; possible assignments include O-bound nitrite, or, more likely,[16] a *nitrato* complex produced by O atom transfer to iron-bound nitrite. Importantly, no spectroscopic evidence consistent with the formation of [Fe(TpivPP)(NO$_2$)] was obtained.

We anticipated that addition of 1 equiv of BF_3·OEt_2 to a chlorobenzene solution of [K(18C6)(OH$_2$)][Fe(TpivPP)(NO$_2$)$_2$] would lead to clean formation of a stable adduct between BF_3 and NO_2^- and the desired five-coordinate complex [Fe(TpivPP)(NO$_2$)]. The reaction of [K(18C6)(OH$_2$)][Fe(TpivPP)(NO$_2$)$_2$] with BF_3·OEt_2 was initially studied at room temperature; the EPR spectra of reaction mixture aliquots indicated the coexistence of several products, including a high-spin species ($g_\perp$ = 5.6), a nitrosyl species ($g \approx 2.01$), and a new rhombic low-spin iron(III) species ($g_1 = 2.60$, $g_2 = 2.37$). To differentiate spectroscopically between this new low-spin species and the low-spin starting material ([Fe(TpivPP)(NO$_2$)$_2$]$^-$ with $g_1 = 2.7$, $g_2 = 2.5$, and $g_3 = 1.6$), subsequent reactions of [K(18C6)(OH$_2$)][Fe(TpivPP)(NO$_2$)$_2$] with BF_3·OEt_2 were studied at ~2 °C to slow the rate of transformation of starting material to products.

Reaction of [K(18C6)(OH$_2$)][Fe(TpivPP)(NO$_2$)$_2$] with BF_3·OEt_2. Selected X-band EPR spectra showing the changes in iron porphyrin species during the reaction of [K(18C6)(OH$_2$)][Fe(TpivPP)(NO$_2$)$_2$] with BF_3·OEt_2 (1.3 molar equiv) in chlorobenzene are shown in Figure 1. The dominant species at ~3 min is the rhombic low-spin starting material, [Fe(TpivPP)(NO$_2$)$_2$]$^-$, as evidenced by the three g values 2.70 (g_1), 2.50 (g_2), and 1.57 (g_3).[21] However, a new low-spin species with $g_2 = 2.36$ and $g_3 = 1.75$ is also evident. A high-spin species with $g_\perp = 5.50$ indicates formation of a second product, while the feature at $g \sim 2$ suggests formation of a third product, a nitrosyl species.

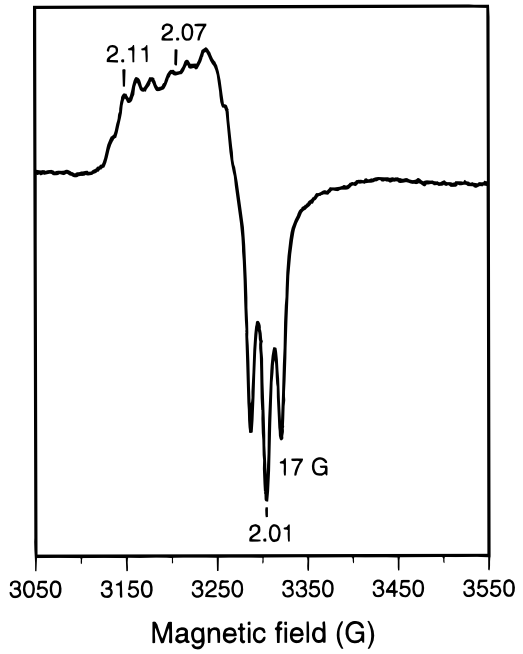

Figure 2. X-band EPR spectrum of the nitrosyl product produced in the reaction between [K(18C6)(OH$_2$)][Fe(TpivPP)(NO$_2$)$_2$] and BF_3·OEt_2 after 2.7 h in chlorobenzene at ~2 °C.

After 21 min, the concentrations of the three product species have increased at the expense of the starting material; the new low-spin species clearly has a rhombic EPR spectrum with $g_1 = 2.60$, $g_2 = 2.35$, and $g_3 = 1.75$. The signal at $g \sim 2$ is sufficiently resolved to reveal a three-line hyperfine splitting pattern, while the signal from the high-spin species ($g_\perp = 5.61$) is broad and exhibits a low-field shoulder ($g \sim$ 6.8).

After 2.7 h, the signal from [Fe(TpivPP)(NO$_2$)$_2$]$^-$ is weaker than that from the new rhombic low-spin species. Both the high-spin product ($g_\perp = 5.68$) and the species characterized by the $g \sim 2$ signal appear to have increased in concentration; an expansion of the high-field signal (Figure 2) clearly indicates that the third product has a near-rhombic g tensor with g_1 = 2.11 ($a_1 \approx 14$ G), $g_2 \approx 2.07$ ($a_2 \approx 21$ G), and $g_3 = 2.01$ ($a_3 \approx$ 17 G). The three-line splitting pattern of the g_3 signal is strong evidence for a hyperfine interaction involving a single ^{14}N nucleus.[33] Since the g values and hyperfine coupling constants match those previously reported for [Fe(TpivPP)(NO)] in chlorobenzene at 77 K[32] and are similar to those reported by Wayland and Olson for [Fe(TPP)(NO)],[34] [Fe(TpivPP)(NO)] is clearly formed in the reaction. This assignment is further supported by the IR spectrum of the reaction mixture taken under argon after 26 h which shows an N≡O stretching band at 1655 cm^{-1}, consistent with the value of ν(NO) observed for solid samples (KBr mulls) of [Fe(TpivPP)(NO)] (1665 cm^{-1})[32] and [Fe(TPP)(NO)] (1670 cm^{-1})[35] and the values of ν(NO)

(32) Nasri, H.; Haller, K. J.; Wang, Y.; Huynh, B. H.; Scheidt, W. R. *Inorg. Chem.* **1992**, *31*, 3459.
(33) Palmer, G. In *Iron Porphyrins*; Physical Bioinorganic Chemistry Series; Lever, A. B. P., Gray, H. B., Eds.; Addison-Wesley: Reading, MA, 1983; Part 2, pp 43−88.
(34) Wayland, B. B.; Olson, L. W. *J. Am. Chem. Soc.* **1974**, *96*, 6037.
(35) Scheidt, W. R.; Frisse, M. E. *J. Am. Chem. Soc.* **1975**, *97*, 17.

recently reported by Bohle and Hung[36] for several five-coordinate (nitrosyl)(porphinato)iron(II) complexes (1675−1705 cm^{-1}).

At long times (t = 25.7 h), the EPR signal from $[Fe(TpivPP)(NO_2)_2]^-$ is not observable, leaving only the new rhombic low-spin species (as a minor component), the high-spin product ($g_\perp = 5.68$), and the species displaying the ^{14}N hyperfine interaction at $g \sim 2$ ([Fe(TpivPP)(NO)]). This product distribution, with the new rhombic low-spin species remaining as a minor component, is observed at t_∞ under argon. Three possible assignments for the high-spin iron(III) product include (i) a five-coordinate N-bound *nitro* complex, (ii) a five-coordinate O-bound *nitrito* complex, and (iii) a mono- or bidentate *nitrato* complex. Since the IR spectrum of the reaction mixture shows three discrete bands at 1520 cm^{-1} (s), 1250 cm^{-1} (m), and 1047 cm^{-1} (m), and the IR spectrum of $[Fe(TpivPP)(NO_2)_2]^-$ (with both nitro ligands N-bound) exhibits two NO_2^- stretching modes at 1351 and 1315 cm^{-1},[21] a five-coordinate N-bound nitro complex can be ruled out. Furthermore, since $[Fe^{II}(TpivPP)(NO_2)]^-$ is known to be low-spin,[37] NO_2^- is likely to form a low-rather than a high-spin complex in the iron(III) derivative. Nitrito complexes of transition metal ions normally show two well-separated stretching modes, ν(N═O) and ν(N−O), at 1485−1400 and 1110−1050 cm^{-1}, respectively.[38] Since the three bands observed for the high-spin reaction product are inconsistent with these modes, linkage isomerism of NO_2^- does not account for the IR data. The three IR bands are in fact consistent with the three stretching modes expected for C_{2v} *nitrate* bound in a bidentate manner to the metal.[38,39] Moreover, the two highest frequency bands are close in energy to those reported by Goff and co-workers for [Fe(TPP)(NO_3)] (1544 and 1275 cm^{-1}).[40] This suggests that the high-spin product of the reaction is [Fe(TpivPP)(NO_3)].

The reaction of $[K(18C6)(OH_2)][Fe(TpivPP)(NO_2)_2]$ and $BF_3{\cdot}OEt_2$ follows a similar course in methylene chloride (Figure S1). However, the formation of the transient rhombic low-spin intermediate proceeds more rapidly so that it is the dominant species in solution after 3 min. The signal due to this species then decays slowly, with a concomitant increase in the signal from the high-spin product ($g_\perp = 5.62$) and the nitrosyl species ($g \approx 2.07$). The EPR spectrum of the reaction mixture after 73 h indicates that a small amount of the low-spin intermediate remains. (The spectrum is similar to that obtained after 25.7 h in chlorobenzene.) Interestingly, the low field signal ($g \approx 5.6$) from [Fe(TpivPP)(NO_3)] is sharper in methylene chloride than in chlorobenzene, mainly as a result of the absence of the shoulder at $g \approx 6.8$.[41]

The EPR spectra of Figure 1 clearly indicate that [Fe(TpivPP)(NO)] and [Fe(TpivPP)(NO_3)] are generated early on in the reaction. A possible pathway by which $[Fe(TpivPP)(NO_2)_2]^-$ reacts with BF_3 to form [Fe(TpivPP)(NO)] and [Fe(TpivPP)(NO_3)] is shown in eqs 1 and 2.

$$[Fe^{III}(TpivPP)(NO_2)_2]^- + BF_3{\cdot}OEt_2 \rightarrow [Fe^{III}(TpivPP)(NO_2)] + [BF_3NO_2]^- \quad (1)$$

$$2[Fe^{III}(TpivPP)(NO_2)] \rightarrow [Fe^{III}(TpivPP)(NO_3)] + [Fe^{II}(TpivPP)(NO)] \quad (2)$$

In the first step, $BF_3{\cdot}OEt_2$ acts as a competing Lewis acid for one of the nitrite ligands of $[Fe(TpivPP)(NO_2)_2]^-$, leading to the formation of a new low-spin mono(nitro)iron(III) complex and a BF_3−nitrite adduct. Although we have no direct experimental evidence that the NO_2^- ion is N-bound in this iron porphyrin intermediate, three factors are consistent with this notion: (i) NO_2^- is N-bound in the analogous *low-spin* iron(II) complex, [K(222)][Fe(TpivPP)(NO_2)],[37] (ii) five-coordinate iron(III) porphyrins with a single O donor axial ligand are usually high-spin[42−52] or admixed-spin ($S = {}^3/_2, {}^5/_2$)[53,54] species, rather than low-spin species, and (iii) a crystal field analysis of the EPR spectrum[55] yields relative crystal field splittings of $\Delta/\lambda = 3.13$ (tetragonality) and $V/\Delta = 0.997$ (rhombicity). The decrease in rhombicity from $V/\Delta = 1.34$[32] in $[Fe(TpivPP)(NO_2)_2]^-$ is consistent with an N-bound mono(nitro) complex.

However, $[Fe^{III}(TpivPP)(NO_2)]$ is a reactive species. In the solvents used (chlorobenzene, CH_2Cl_2, and DMF), $[Fe^{III}(TpivPP)(NO_2)]$ converts into [Fe(TpivPP)(NO)] and [Fe(TpivPP)(NO_3)] (eq 2), consistent with the EPR and IR spectral data. Furthermore, $[Fe(TpivPP)(NO_2)_2]^-$ in chlorobenzene solution (*vide infra*) reacts to give the same products under an argon atmosphere. The ratio of [Fe(TpivPP)(NO_3)] to [Fe(TpivPP)(NO)] produced in the reaction of $[Fe(TpivPP)(NO_2)_2]^-$ with $BF_3{\cdot}OEt_2$ appears to be solvent dependent. Apparently

(36) Bohle, S. D.; Hung, C.-H. *J. Am. Chem. Soc.* **1995**, *117*, 9584.
(37) Nasri, H.; Wang, Y.; Huynh, B. H.; Scheidt, W. R. *J. Am. Chem. Soc.* **1991**, *113*, 717.
(38) Nakamoto, K. *Infrared and Raman Spectra of Inorganic and Coordination Compounds*, 3rd ed.; Academic: New York, 1977; pp 244−247.
(39) The large separation of the two highest frequency bands (270 cm^{-1}) is consistent with a symmetric bidentate NO_3^- complex;[38] smaller separations are observed for unidentate nitrato complexes such as the monoclinic form of [Fe(OEP)(ONO_2)] which shows three NO_3^- modes at 1515, 1385, and 1276 cm^{-1} (Munro, O. Q.; Scheidt, W. R. Unpublished results).
(40) Phillippi, M. A.; Baenziger, N.; Goff, H. M. *Inorg. Chem.* **1981**, *20*, 3904.
(41) The changes in the EPR spectrum of the reaction mixture initially comprising $[K(18C6)(OH_2)][Fe(TpivPP)(NO_2)_2]$ and $BF_3{\cdot}OEt_2$ in DMF at 2 °C were less well resolved. However, clear evidence for the formation of the high-spin species ($g_\perp = 5.68$) and a nitrosyl species ($g \sim 2$) within the first 3 min of the reaction was obtained. The signal from the rhombic low-spin starting material, $[Fe(TpivPP)(NO_2)_2]^-$, had $g_1 = 2.74$, $g_2 = 2.47$, and $g_3 = 1.67$ in DMF. The broad, asymmetric shape of the g_1 signal obtained from $[Fe(TpivPP)(NO_2)_2]^-$ suggested that signals from two low-spin iron(III) species were overlapped in this region of the spectrum. After 3 h, the high-spin product ($g_\perp = 5.68$) had a sharp derivative signal which appeared larger than the g_1 feature from the low-spin starting material and the (nitrosyl)iron(II) signal. In contrast to the reaction in chlorobenzene or methylene chloride, the signal from the nitrosyl product never became the most intense spectral feature, even after 5 h.
(42) Lecomte, C.; Chadwick, D. L.; Coppens, P.; Stevens, E. D. *Inorg. Chem.* **1983**, *22*, 2982.
(43) Goff, H. M.; Shimomura, E. T.; Lee, Y. J.; Scheidt, W. R. *Inorg. Chem.* **1984**, *23*, 315.
(44) Cocolios, P.; Lagrange, G.; Guilard, R.; Oumous, H.; Lecomte, C. *J. Chem. Soc., Dalton Trans.* **1984**, 567.
(45) Scheidt, W. R.; Lee, Y. J.; Finnegan, M. G. *Inorg. Chem.* **1988**, *27*, 4725.
(46) Hatano, K.; Uno, T. *Bull. Chem. Soc. Jpn.* **1990**, *63*, 1825.
(47) Helms, A. M.; Jones, W. D.; McLendon, G. L. *J. Coord. Chem.* **1991**, *23*, 351.
(48) Gonzales, J. A.; Wilson, L. J. *Inorg. Chem.* **1994**, *33*, 1543.
(49) Cheng, B.; Hobbs, J. D.; Debrunner, P. G.; Erlebacher, J.; Shelnutt, J. A.; Scheidt, W. R. *Inorg. Chem.* **1995**, *34*, 102.
(50) Bohle, D. S.; Conklin, B. J.; Hung, C.-H. *Inorg. Chem.* **1995**, *34*, 2569.
(51) Hoffman, A. B.; Collins, D. M.; Day, V. W.; Fleischer, E. B.; Srivastava, T. S.; Hoard, J. L. *J. Am. Chem. Soc.* **1972**, *94*, 3620.
(52) Lay, K. L.; Buchler, J. W.; Kenny, J. E, Scheidt, W. R. *Inorg. Chim. Acta* **1986**, *123*, 91.
(53) Reed, C. A.; Mashiko, T.; Bentley, S. P.; Kastner, M. E.; Scheidt, W. R.; Spartalian, K.; Lang, G. *J. Am. Chem. Soc.* **1979**, *101*, 2948.
(54) Masuda, H.; Taga, T.; Osaki, K.; Sugimoto, H.; Yoshida, Z.-I.; Ogoshi, H. *Inorg. Chem.* **1980**, *19*, 950.
(55) Taylor, C. P. S. *Biochim. Biophys. Acta* **1977**, *491*, 137. We have assumed that "*z*" is along the heme normal.

differing nitrate/nitrosyl ratios were observed in chlorobenzene (Figure 1 and CH_2Cl_2 (Figure S1). Since colorless crystals of $[K(18C6)][BF_3{\cdot}NO_3]$ were isolated[56] along with crystals of $[Fe(TpivPP)(NO_3)]$, a third reaction (eq 3) apparently competes with eq 2 for $[Fe^{III}(TpivPP)(NO_2)]$ to form $[Fe^{II}(TpivPP)(NO)]$.

$$[Fe^{III}(TpivPP)(NO_2)] + [BF_3{\cdot}NO_2]^- \rightarrow [Fe^{II}(TpivPP)(NO)] + [BF_3{\cdot}NO_3]^- \quad (3)$$

Oxygen atom transfer from iron-bound nitrite to free NO_2^- is well-known[16] and appears to be favored to some extent here, particularly in chlorobenzene.

Importantly, eqs 2 and 3, i.e., oxygen atom transfer from $[Fe^{III}(TpivPP)(NO_2)]$, are consistent with (i) the tendency of related $Ru^{III}-NO_2$ complexes to undergo O atom transfer to produce $Ru^{III}-NO_3$ and $Ru^{II}-NO$,[57] (ii) our previous spectroscopic observations that $[Fe^{III}(TPP)(NO_2)]$ readily forms $[Fe^{II}(TPP)(NO)]$ in the presence of an O atom acceptor such as free nitrite ion,[16] and (iii) the recent findings of Castro and co-workers[17] that [Fe(OEP)Cl] stoichiometrically oxidizes both inorganic and organic substrates in the presence of a slight excess of nitrite ion.[58] The general significance of eqs 2 and 3 is that studies aimed at using or characterizing five-coordinate nitro complexes of iron(III) porphyrins are likely to be hampered by the inherent instability of this species.

Oxidation Studies. Nitric oxide complexes of iron(II) porphyrins are relatively unstable under aerobic conditions, being oxidized by dioxygen to the corresponding iron(III) nitrates.[16] In the case of hemoproteins such as MbNO, dioxygen reacts with coordinated NO to give an N-bound peroxynitrite intermediate which then decays to metMbNO_3.[7] $[Fe(TpivPP)(NO)]$ produced in the reaction of $[K(18C6)(OH_2)][Fe(TpivPP)(NO_2)_2]$ with $BF_3{\cdot}OEt_2$ under argon could be removed by oxidation over a period of ~60 h at 40 °C with gaseous oxygen. X-band EPR spectra of aliquots from the reaction in chlorobenzene are shown in Figure 3. Three significant time-dependent changes are evident: (i) the signal due to $[Fe(TpivPP)(NO)]$ centered at $g \sim 2.07$ decays with time, (ii) the signal characteristic of the low-spin iron(III) intermediate *increases* in intensity before diminishing to zero as the reaction approaches completion, and (iii) the signal at low field from $S = {}^5/_2$ $[Fe(TpivPP)(NO_3)]$ ($g_\perp = 5.84$) increases in intensity until it is the principal component after 36 h. The growth and subsequent decay of the rhombic low-spin iron(III) EPR signal suggests that a porphyrin intermediate is produced upon oxidation of $[Fe(TpivPP)(NO)]$ and ultimately consumed in the formation of $[Fe(TpivPP)(NO_3)]$. Since the g values of this intermediate match those of $[Fe(TpivPP)(NO_2)]$ (Figure 1), a simple scheme which qualitatively accounts for the principal species observed during the oxidation of $[Fe(TpivPP)(NO)]$ is given in eqs 4 and 5.

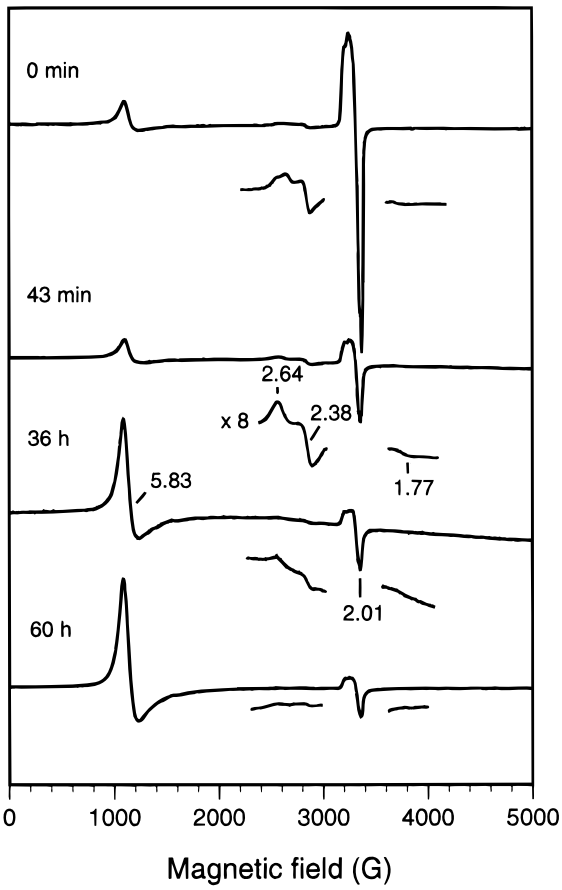

Figure 3. Selected X-band EPR spectra showing oxidation (40 °C, chlorobenzene) of the compound characterized by a ^{14}N hyperfine-split signal centered at $g \sim 2.07$. The starting solution contains the two products of the anaerobic reaction of $[K(18C6)(OH_2)][Fe(TpivPP)(NO_2)_2]$ and $BF_3{\cdot}OEt_2$ at t_∞ as well as some residual $[Fe(TpivPP)(NO_2)]$.

$$2[Fe^{II}(TpivPP)(NO)] + O_2 \rightarrow 2[Fe^{III}(TpivPP)(NO_2)] \quad (4)$$

$$2[Fe^{III}(TpivPP)(NO_2)] \rightarrow [Fe^{III}(TpivPP)(NO_3)] + [Fe^{II}(TpivPP)(NO)] \quad (5)$$

The $Fe^{II}-NO$ complex produced in the second step (eq 5) is then reoxidized until conversion to $[Fe(TpivPP)(NO_3)]$ is complete. The EPR spectra shown in Figure 3 indicate that the final product of the reaction is $[Fe(TpivPP)(NO_3)]$, which is readily crystallized from chlorobenzene. Oxidation of $[Fe(TpivPP)(NO)]$ is considerably slower than oxidation of $[Fe(TPP)(NO)]$,[16] consistent with coordination and steric protection of NO within the pocket of the porphyrin.[32] Alternatively, the NO in-pocket/out-of-pocket equilibration rate could be slow.

Oxidation of metallonitrosyls to nitro complexes is not unprecedented. For example, Clarkson and Basolo[59] have shown that the mechanism of oxidation of several $Co^{II}-NO$ salen analogues is first order in both metal nitrosyl and oxygen and leads to the formation of an N-bound peroxynitrite intermediate. This species rapidly attacks a second metal

(56) The IR spectrum (KBr mull) of colorless crystals of $[K(18C6)][BF_3{\cdot}NO_3]$ showed diagnostic absorption bands at 2922, 2856, and 1493 cm^{-1} (m, $-CH_2-$), 1733 cm^{-1} (br, B−O), 1385 cm^{-1} (s, NO_3^-), 1105 cm^{-1} (s, CH_2-O-CH_2), and 962 cm^{-1} (m, B−F). The K(18C6) and NO_3^- modes assigned here are in good agreement with those reported for the structurally characterized (2*S*,6*S*)-2,6-dimethyl-1,4,7,-10,13,16-hexaoxacyclooctadecane complex of KNO_3 (Dyer, R. B.; Ghirardelli, R. G.; Palmer, R. A.; Holt, E. M. *Inorg. Chem.* **1986**, *25*, 3184).

(57) (a) Keene, F. R.; Salmon, D. J.; Meyer, T. J. *J. Am. Chem. Soc.* **1977**, *99*, 2384. (b) Keene, F. R.; Salmon, D. J.; Walsh, J. L.; Abruner, H. D.; Meyer, T. J. *J. Am. Chem. Soc.* **1977**, *99*, 4821. (c) Keene, F. R.; Salmon, D. J.; Walsh, J. L.; Abruner, H. D.; Meyer, T. J. *Inorg. Chem.* **1980**, *19*, 1896.

(58) Depending on the values of K_1 and K_2 for nitrite coordination by [Fe(OEP)Cl] in *N*-methylpyrrolidone−1% acetic acid solution, a slight excess (2−4 molar equiv)[17] of $[K(18C6)][NO_2]$ presumably results in a significant fraction of the reactive five-coordinate mono(nitro) species, $[Fe(OEP)(NO_2)]$, in addition to the six-coordinate bis(nitro) complex.

(59) (a) Clarkson, S. G.; Basolo, F. *Inorg. Chem.* **1973**, *12*, 1528. (b) Clarkson, S. G.; Basolo, F. *J. Chem. Soc., Chem. Commun.* **1972**, 670.

nitrosyl to form an unstable peroxo-bridged intermediate (N−O−O−N) which decomposes to the nitro complex.

EPR Study of the Decomposition of [K(18C6)(OH$_2$)][Fe(TpivPP)(NO$_2$)$_2$]. An initially 2.52 mM chlorobenzene solution of [K(18C6)(OH$_2$)][Fe(TpivPP)(NO$_2$)$_2$] was investigated by periodically withdrawing samples, freezing, and running the EPR spectrum.[60] The EPR spectrum of the solution 3.5 min after dissolution indicated formation of three new species; a high-spin species with $g_\perp = 5.64$, a rhombic low-spin species ($g_1 = 2.60$, $g_2 = 2.36$, and $g_3 = 1.77$) spectroscopically distinct from the starting material ($g_1 = 2.70$, $g_2 \approx 2.5$, and $g_3 = 1.56$), and a species with a three-line ^{14}N hyperfine-split signal at $g \sim 2.01$. The intensities of the product signals increased with time (as in the reaction with BF$_3$·OEt$_2$); after 7.5 min, the most intense signal centered at $g \sim 2.08$ had a similar ^{14}N hyperfine splitting pattern to that observed in the reaction of [K(18C6)(OH$_2$)][Fe(TpivPP)(NO$_2$)$_2$] with BF$_3$·OEt$_2$ (Figure 2). The g values (and hyperfine coupling constants) of this product were $g_1 \approx 2.11$ ($a_1 \approx 14$ G), $g_2 \approx 2.08$ ($a_2 \approx 24$ G), and $g_3 = 2.01$ ($a_3 \approx 17$ G). The spectrum of the solution after 28 h at room temperature was similar to that shown in Figure 1 for the product mixture generated with BF$_3$·OEt$_2$ after 25.7 h at 2 °C. These observations suggest that partial dissociation of nitrite ion from the bis(nitro) complex affords [Fe(TpivPP)(NO$_2$)], which undergoes oxygen atom transfer to yield [Fe(TpivPP)(NO$_3$)] and [Fe(TpivPP)(NO)] as before. In contrast, the synthesis of [K(18C6)(H$_2$O)][Fe(TpivPP)(NO$_2$)$_2$] uses a large excess of NO$_2^-$, which clearly minimizes the concentration of the reactive five-coordinate iron(III) species and allows isolation of the stable bis(nitro) complex.[21] It is noteworthy that [Fe^{II}(TpivPP)(NO$_2$)], unlike the mono(nitro) iron(III) derivative, is stable under anaerobic conditions in chlorobenzene.[37]

Molecular Structure of [Fe(TpivPP)(NO$_3$)]. The identity of the high-spin iron(III) product generated in the reaction of [K(18C6)(OH$_2$)][Fe(TpivPP)(NO$_2$)$_2$] with BF$_3$·OEt$_2$ and in the reaction of [Fe(TpivPP)(NO)] with dioxygen was established unambiguously from low-temperature X-ray diffraction measurements. Figure 4 shows an ORTEP drawing of [Fe(TpivPP)(NO$_3$)]. The nitrate ion occupies the coordination position within the pocket of the porphyrin and is bound to the iron in a near-symmetric bidentate fashion with individual Fe−O distances of 2.226(3) and 2.123(3) Å. Averaged values of the bond distances and bond angles within the porphyrin core are shown in Figure 5. Individual values of bond distances and angles for [Fe(TpivPP)(NO$_3$)] are given in the Supporting Information, and selected bond lengths and angles within the coordination group are shown in Table 2.

As shown in Figure 6, the dihedral angles between the plane of the axial nitrato ligand and the N(1)−Fe−N(3) and N(2)−Fe−N(4) planes are 10.0 and 80.3°, respectively; the coordinating nitrate oxygens are thus positioned approximately above the N(1)−Fe and N(3)−Fe bonds. The mean plane of the nitrate ion is essentially orthogonal (89.1°) to the 24-atom porphyrin mean plane. The trans N$_p$−Fe−N$_p$ angles are significantly different, with N(1)−Fe−N(3) = 146.14(9)° and N(2)−Fe−N(4) = 154.84(9)° (Table 2). Commensurate differences in the Fe−N$_p$ bond distances are observed; those involving the more acute angle (N(1)−Fe−N(3)) average 2.083(3) Å and are longer

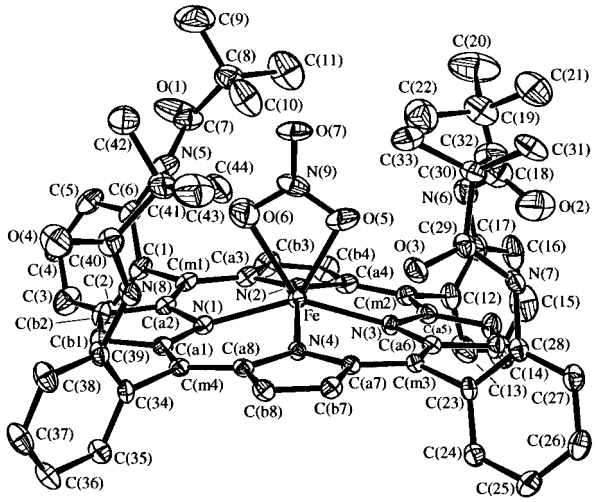

Figure 4. ORTEP diagram showing a labeled edge-on view of the structure of [Fe(TpivPP)(NO$_3$)] (50% probability surfaces). Hydrogen atoms have been omitted for clarity. The near-perpendicular orientation of the bidentate nitrato ligand relative to the N(2)−Fe−N(4) plane is clearly evident (the dihedral angle is 80.3°).

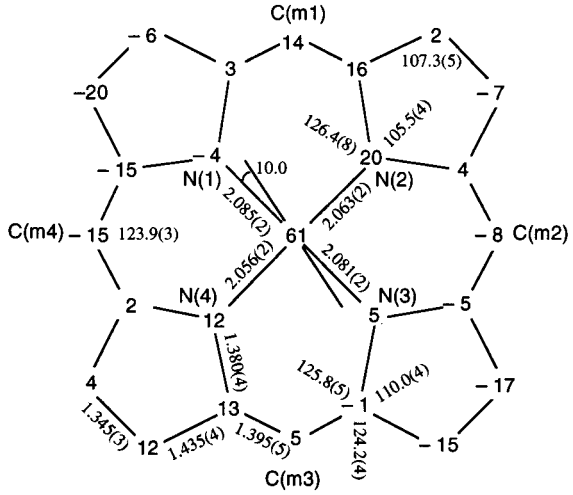

Figure 5. Formal diagram of the porphinato core of [Fe(TpivPP)(NO$_3$)] illustrating the displacement of each unique atom (in units of 0.01 Å) from the mean plane of the 24-atom core. Positive values of displacement are toward the axial nitrato ligand. Also shown on the diagram are the averaged values of each chemically unique class of bond distance and angle in the porphinato core. The orientation of the axial nitrato ligand and individual Fe−N$_p$ bond distances are indicated.

(by ∼4 standard deviations) than those involving the more obtuse angle which average 2.060(5) Å. This distortion of the coordination geometry apparently reflects both the bidentate mode of nitrate coordination and the orientation of the axial ligand relative to the Fe−N$_p$ bonds.

The iron(III) ion is displaced 0.61 Å from the 24-atom mean plane of the porphyrin core toward the axial nitrato ligand (Figure 5). The porphinato core displays a combination of doming and S_4 ruffling as evidenced by (i) the tilt of the four pyrrole rings relative to the porphyrin mean plane (5.6, 6.6, 5.5, and 3.1° for the rings containing N(1) to N(4), respectively) and (ii) the displacement of the *meso*-carbons alternately above and below the porphyrin mean plane (Figure 5). The dihedral angles between the *meso*-phenyl groups and the porphyrin mean plane are 70.7, 82.7, 72.0, and 81.6° for the phenyl rings attached to *meso*-carbons 1 to 4, respectively. Figure 6 shows that the amide groups of the pivalamido substituents are not coplanar

(60) The solution of [K(18C6)(OH$_2$)][Fe(TpivPP)(NO$_2$)$_2$] used for this study was prepared by rapidly dissolving ground crystals of [K(18C6)(OH$_2$)][Fe(TpivPP)(NO$_2$)$_2$] in chlorobenzene under argon; the solution therefore does not contain an excess of NO$_2^-$, unlike solutions used for growing crystals of [K(18C6)(OH$_2$)][Fe(TpivPP)(NO$_2$)$_2$] from chlorobenzene and hexane.[21]

Table 2. Selected Bond Lengths and Angles for [Fe(TpivPP)(NO_3)][a]

(A) Bond Lengths

Fe−N(1)	2.085(2)	Fe−N(2)	2.063(2)
Fe−N(3)	2.081(2)	Fe−N(4)	2.056(2)
Fe−O(5)	2.123(3)	Fe−O(6)	2.226(3)
N(9)−O(5)	1.271(4)	N(9)−O(6)	1.252(4)
N(9)−O(7)	1.214(3)		

(B) Bond Angles

N(1)−Fe−N(2)	86.54(9)	N(1)−Fe−N(3)	146.14(9)
N(1)−Fe−N(4)	86.28(9)	N(2)−Fe−N(3)	86.34(9)
N(2)−Fe−N(4)	154.85(9)	N(3)−Fe−N(4)	86.29(9)
N(4)−Fe−O(5)	97.70(10)	N(2)−Fe−O(5)	104.68(10)
N(3)−Fe−O(5)	80.20(10)	N(1)−Fe−O(5)	133.56(10)
N(4)−Fe−O(6)	106.66(10)	N(2)−Fe−O(6)	95.06(10)
N(3)−Fe−O(6)	136.93(9)	N(1)−Fe−O(6)	76.70(9)
O(5)−Fe−O(6)	57.75(10)	N(9)−O(5)−Fe	92.5(2)
N(9)−O(5)−Fe	96.9(2)	O(7)−N(9)−O(5)	112.8(3)
O(7)−N(9)−O(5)	123.1(3)	O(7)−N(9)−O(6)	124.0(3)

[a] The estimated standard deviations of the least-significant digits are given in parentheses.

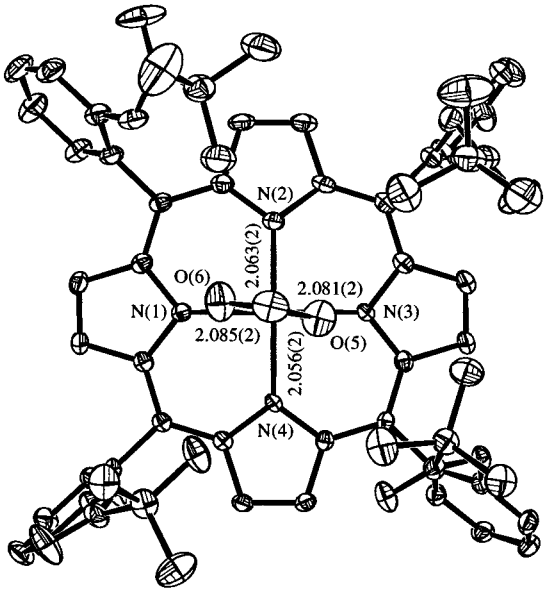

Figure 6. ORTEP diagram showing the structure of [Fe(TpivPP)(NO_3)] (50% probability surfaces) looking down the heme normal from the same side as the axial nitrato ligand. Hydrogen atoms have been omitted for clarity. The dihedral angle between the axial ligand and N(2)−Fe−N(4) planes is 10.0°.

with the phenyl rings to which they are bonded; the individual dihedral angles are 35.5, 80.1, 58.6, and 16.1° for the amide linkages of phenyl rings 1 to 4, respectively. The *o*-pivalamido group of the phenyl ring attached to C(m1) is disordered, displaying two orientations relative to the plane of the phenyl group, apparently as a result of rotation about the C(6)−N(5) bond. The dihedral angle between the amide group of the major component (84%) and the minor component (16%) is 61.4°. An ORTEP diagram showing the minor component of the disordered group is given in the Supporting Information (Figure S2).

The structure of [Fe(TpivPP)(NO_3)] is unusual in several respects. Although bidentate coordination of nitrate is known for [Fe(TPP)(NO_3)],[40] the plane of the nitrate ion in the TPP derivative bisects an opposite pair of cis N_p−Fe−N_p angles. The acute nitrate orientation (10°) observed in [Fe(TpivPP)(NO_3)] is clearly more akin to the eclipsing orientations (0°) found for the bidentate peroxo ligands of [Ti(OEP)(O_2)],[61] [K(K222)][Mn(TPP)(O_2)],[62] and [Mo(TTP)(O_2)$_2$].[63] The nitrate orientation in [Fe(TpivPP)(NO_3)] apparently leads to the statistically significant difference between the N(1)−Fe−N(3) and N(2)−Fe−N(4) angles. This distortion of the coordination sphere geometry is also observed in the two nominally five-coordinate peroxo complexes, [Ti(OEP)(O_2)][61] and [K(K222)][Mn(TPP)(O_2)].[62] Interestingly, the short Fe−N_p distances observed for the bonds perpendicular to the nitrate ion in [Fe(TpivPP)(NO_3)] parallel the coordination geometry in [Ti(OEP)(O_2)][61] but not that in [Mn(TPP)(O_2)]$^-$,[62] which shows the reverse pattern (long Mn−N_p bonds perpendicular to the Mn−peroxo plane).

Currently, there are four structurally characterized (nitrato)(porphinato)iron(III) complexes: [Fe(TpivPP)(NO_3)], [Fe(TPP)(NO_3)],[40] triclinic [Fe(OEP)(NO_3)],[64] and a monoclinic form of [Fe(OEP)(NO_3)].[65] All have unique nitrate coordination geometries. These range from "symmetric" monodentate in the monoclinic form of [Fe(OEP)(NO_3)][65] to "symmetric" bidentate in [Fe(TpivPP)(NO_3)]. This changing mode of nitrate coordination is accompanied by an increase in the out-of-plane displacement of the iron(III) ion (0.45 → 0.61 Å) and a concomitant increase in the mean Fe−N_p bond distance from 2.047(6) Å in monoclinic [Fe(OEP)(NO_3)] to 2.071(14) Å in [Fe(TpivPP)(NO_3)]. The Fe−N_p bonds become more asymmetric as the mode of nitrate coordination switches from mono- to bidentate. Each species has a unique EPR spectrum which is apparently related to the symmetry of the iron(III) center; the complete electronic structures of these species are currently under investigation and will be reported elsewhere.

Conclusions

The reaction of [K(18C6)(OH_2)][Fe(TpivPP)(NO_2)$_2$] with BF_3·OEt_2 under argon leads to the formation of a new low-spin iron(III) porphyrin species assigned on the basis of its EPR spectrum in several solvents as the N-bound mono(nitro) complex, [Fe(TpivPP)(NO_2)]. This five-coordinate iron(III) nitro species is, however, reactive and readily transfers an oxygen atom to form [Fe^{II}(TpivPP)(NO)] and [Fe^{III}(TpivPP)(NO_3)]. The low-temperature X-ray structure of [Fe(TpivPP)(NO_3)] shows that the nitrate ion is bound within the pocket of the porphyrin in a near-symmetric bidentate fashion in which the coordinating oxygens are positioned approximately over a trans pair of Fe−N_p bonds. This mode of nitrate coordination considerably lowers the symmetry of the iron(III) center.

Acknowledgment. We thank the National Institutes of Health for support of this research under Grant GM-38401 (W.R.S). Funds for the purchase of the FAST area detector diffractometer were provided through NIH Grant RR-06709. We thank Dr. G. J. Ferraudi of the Radiation Laboratory (University of Notre Dame) for the use of the Bruker EPR spectrometer.

(61) Guilard, R.; Latour, J.-C.; Lecomte, C.; Marchon, J.-C.; Protas, J.; Ripoll, D. *Inorg. Chem.* **1978**, *17*, 1228.
(62) VanAtta, R. B.; Strouse, C. E.; Hanson, L. K.; Valentine, J. S. *J. Am. Chem. Soc.* **1987**, *109*, 1425.
(63) Chevrier, B.; Diebold, T.; Weiss, R. *Inorg. Chim. Acta* **1976**, *19*, L57.
(64) Ellison, M. K.; Shang, M.; Kim, J.; Scheidt, W. R. *Acta Crystallogr., Sect. C* **1996**, *C52*, 3040.
(65) The monoclinic form of [Fe(OEP)(NO_3)] has an Fe−O distance of 1.966(2) Å and a mean Fe−N_p distance of 2.047(6) Å; the iron(III) ion is displaced 0.45 Å from the 24-atom porphyrin mean plane. (Munro, O. Q.; Scheidt, W. R. Unpublished results.).

Supporting Information Available: Complete crystallographic details, atomic coordinates, anisotropic thermal parameters, fixed hydrogen atom coordinates, bond lengths, and bond angles for [Fe(TpivPP)(NO_3)] (Tables S1−S6); X-band EPR spectra following the reaction of [K(18C6)(OH_2)][Fe(TpivPP)(NO_2)$_2$] and BF_3·OEt_2 in CH_2Cl_2 (Figure S1); and an ORTEP diagram of [Fe(TpivPP)(NO_3)] showing the rotational disorder of one *o*-pivalamido group (Figure S2) (18 pages). An X-ray crystallographic file, in CIF format, is available on the Internet only. Ordering and access information is given on any current masthead page.

IC970855L